



Trans. Nonferrous Met. Soc. China 24(2014) 406-414

Transactions of Nonferrous Metals Society of China

www.tnmsc.cn

Structures and electrochemical hydrogen storage performance of Si added A₂B₇-type alloy electrodes

Yang-huan ZHANG^{1,2}, Hui-ping REN¹, Ying CAI¹, Tai YANG^{1,2}, Guo-fang ZHANG^{1,2}, Dong-liang ZHAO²

- 1. Key Laboratory of Integrated Exploitation of Baiyun Obo Multi-Metal Resources, Inner Mongolia University of Science and Technology, Baotou 014010, China;
- 2. Department of Functional Material Research, General Iron and Steel Research Institute, Beijing 100081, China

Received 4 January 2013; accepted 6 September 2013

Abstract: In order to ameliorate the electrochemical hydrogen storage performance of La–Mg–Ni system A_2B_7 -type electrode alloys, a small amount of Si was added. The La_{0.8}Mg_{0.2}Ni_{3.3}Co_{0.2}Si_x(x=0–0.2) electrode alloys were prepared by casting and annealing. The effects of adding Si on the structure and electrochemical hydrogen storage characteristics of the alloys were investigated systematically. The results indicate that the as-cast and annealed alloys hold multiple structures, involving two major phases of (La, Mg)₂Ni₇ with a Ce₂Ni₇-type hexagonal structure and LaNi₅ with a CaCu₅-type hexagonal structure as well as one residual phase LaNi₃. The addition of Si results in a decrease in (La, Mg)₂Ni₇ phase and an increase in LaNi₅ phase without changing the phase structure of the alloys. What is more, it brings on an obvious effect on electrochemical hydrogen storage characteristics of the alloys. The discharge capacities of the as-cast and annealed alloys decline with the increase of Si content, but their cycle stabilities clearly grow under the same condition. Furthermore, the measurements of the high rate discharge ability, the limiting current density, hydrogen diffusion coefficient as well as electrochemical impedance spectra all indicate that the electrochemical kinetic properties of the electrode alloys first increase and then decrease with the rising of Si content.

Key words: A₂B₇-type electrode alloy; Si additive; structure; electrochemical characteristics

1 Introduction

Some major advantages of the Ni/MH battery, such as high-energy density, excellent power density, as well as long cycle life, make it become a leading technology as the battery power source for electric vehicles (EVS) [1]. However, further improvements of the battery are compulsory for superior performances, especially discharge capacity and electrochemical hydrogen storage kinetics. The rare earth-based AB₅-type alloys, although have been industrialized in a large scale in China and Japan, are suffering from a severe frustration on account of their limited discharge capacity (about 330 mA·h/g). Thus, the demand for new electrode materials with performance has become increasingly imperative. In such circumstance, La-Mg-Ni-system A₂B₇-type alloys are considered to be the most promising candidates as the negative electrode materials of Ni/MH

rechargeable battery in virtue of their higher discharge capacities (380-410 mA·h/g) and lower production costs since KADIR et al [2] and KOHNO et al [3] reported their research results. Huge number of financial supports have been provided by the National High Technology Research and Development Program of China in order to promote the industrialization of these new-type alloys, and to our relief, a promising progress has been obtained in many scientific researchers' hard works as summarized by LIU et al [4,5]. However, the production of the new type alloys as the negative electrode in Ni/MH battery has not been found in China because of little poor electrochemical cycle stability of the electrode alloys. A serious challenge faced by researchers in this field keeps intact, enhancing the cycle stability of the alloy without lowering its discharge capacity.

It was believed that the element substitution is an effective method for improving the overall properties of the hydrogen storage alloys. In the case of La-Mg-Ni

Foundation item: Projects (50961009, 51161015) supported by the National Natural Science Foundation of China; Project (2011AA03A408) supported by the High-tech Research and Development Program of China; Projects (2011ZD10, 2010ZD05) supported by the Natural Science Foundation of Inner Mongolia, China

Corresponding author: Yang-huan ZHANG; Tel: +86-10-62183115; Fax: +86-10-62187102; E-mail: zhangyh59@sina.com DOI: 10.1016/S1003-6326(14)63076-4

series hydrogen-storage alloys, the partial replacement of Ni with Co, Fe, Mn, Al, Cu [6,7] and La with Ce, Pr, Nd [8–11] was studied systematically. Furthermore, it was convinced that the capacity deterioration of the La–Mg–Ni system alloy electrodes is mainly attributed to the pulverization of the alloy particles and the oxidation/corrosion of the elements Mg and La [12]. Therefore, we expect that the addition of Si can strengthen the anti-oxidation and anti-corrosion abilities of the alloy for it will form a compact silicon oxide film on the surface of the alloy electrode. To confirm this, a systematical investigation about the effects of additive Si on the structures and electrochemical hydrogen storage kinetics of the La_{0.8}Mg_{0.2}Ni_{3.3}Co_{0.2}Si_x (x=0–0.2) electrode alloys was carried out.

2 Experimental

The chemical compositions of the electrode alloys were $La_{0.8}Mg_{0.2}Ni_{3.3}Co_{0.2}Si_x$ (x=0–0.2). For convenience, the alloys were denoted with Si content as Si₀, Si_{0.05}, Si_{0.15}, Si_{0.15} and Si_{0.2}, respectively. The alloy ingots were prepared using a vacuum induction furnace in helium atmosphere under the pressure of 0.04 MPa in order to prevent element Mg from volatilizing during the melting. A part of the alloy was annealed at 900 °C for 8 h in vacuum.

The phase structures and compositions of the as-cast and annealed alloys were characterized by XRD (D/max/2400). The diffraction, with the experimental parameters of 160 mA, 40 kV and 10 (°)/min respectively, was performed with Cu $K_{\alpha 1}$ radiation filtered by graphite. The morphologies of the as-cast and as-annealed alloys were examined by SEM (QUANTA 400).

The round electrode pellets with 15 mm in diameter were prepared by cold pressing the mixture of alloy powder and carbonyl nickel powder with the mass ratio of 1:4 under the pressure of 35 MPa. After being dried for 4 h, the electrode pellets were immersed in a 6 mol/L KOH solution for 24 h to wet the electrodes fully before the electrochemical measurement.

The electrochemical measurements were performed at 30 °C using a tri-electrode open cell, consisting of a working electrode (the metal hydride electrode), a sintered Ni(OH)₂/NiOOH counter electrode and a Hg/HgO reference electrode, which were immersed in the electrolyte of 6 mol/L KOH, and the voltage between the negative electrode and the reference one was defined as the discharge voltage. In every cycle, the alloy electrode was first charged with a constant current density. After resting for 15 min, it was discharged with the same current density to cut-off voltage of -0.500 V.

The electrochemical impedance spectra (EIS) and

the Tafel polarization curves of the alloys were measured by electrochemical workstation (PARSTAT 2273). The fresh electrodes were fully charged and then rested for 2 h up to the open circuit potential stabilization. For the EIS measurement, the frequency range was from 10 kHz to 5 mHz at 50% depth of discharge (DOD), the amplitude of signal potentiostatic or galvanostatic measurements was 5 mV, and the number of points per decade of frequencies was 60. For the Tafel polarization curves, the potential range was from -1.2 to 1.0 V (vs Hg/HgO) with a scanning rate of 5 mV/s. For the potentiostatic discharge, the test electrodes in the fully charged state were discharged at 500 mV potential steps for 5000 s on electrochemical workstation (PARSTAT 2273), using the electrochemistry corrosion software (CorrWare).

3 Results and discussion

3.1 Structural characteristics

The XRD patterns of the as-cast and as-annealed $La_{0.8}Mg_{0.2}Ni_{3.3}Co_{0.2}Si_x$ (x=0-0.2) alloys are presented in Fig. 1. It is found by International Centre for Diffraction Data (ICDD) identification that all the as-cast and as-annealed alloys hold a multiphase structure, containing two major phases (La, Mg)₂Ni₇ and LaNi₅ as well as a residual phase LaNi3, which maintains almost unaltered when a small amount of Si was added. The lattice parameters together with the abundances of the major phases (La, Mg)₂Ni₇ and LaNi₅ in the alloys are listed in Table 1 calculated by Jade 6.0 software based on the XRD data. We note that the lattice constants and cell volumes of the two major phases in the alloys visibly enlarge with the rising of Si content, which justifies the successful alloying of Si with (La, Mg)₂Ni₇ and LaNi₅. Differently, the action that an extra element is joined makes the lattice constants of LaNi₅ phase increase much larger than those of (La, Mg)₂Ni₇ phase, indicating that Si atoms are more apt to dissolve into LaNi₅ phase. Also, it is evident that the addition of Si engenders an obvious increase in the LaNi₅ phase and a decrease in the (La, Mg)₂Ni₇ phase, as given in Table 1. Furthermore, it can be seen from Table 1 that the annealing treatment induces a notable increase in the (La, Mg)₂Ni₇ phase and a decrease in the LaNi₅ phase, and it also causes an obvious enlargement in the lattice constants and cell volume of the major phases in the alloys.

The SEM images of the as-cast and as-annealed Si₀ and Si_{0,2} alloys are shown in Fig. 2. The analysis of SEM with energy dispersive spectrometry (EDS) reveals that all the experimental alloys have multiphase structure, containing (La, Mg)₂Ni₇ (denoted as A), LaNi₅ (denoted as B) and LaNi₃ (denoted as C) phases. Moreover, the EDS patterns exhibit that the Si content in the LaNi₅

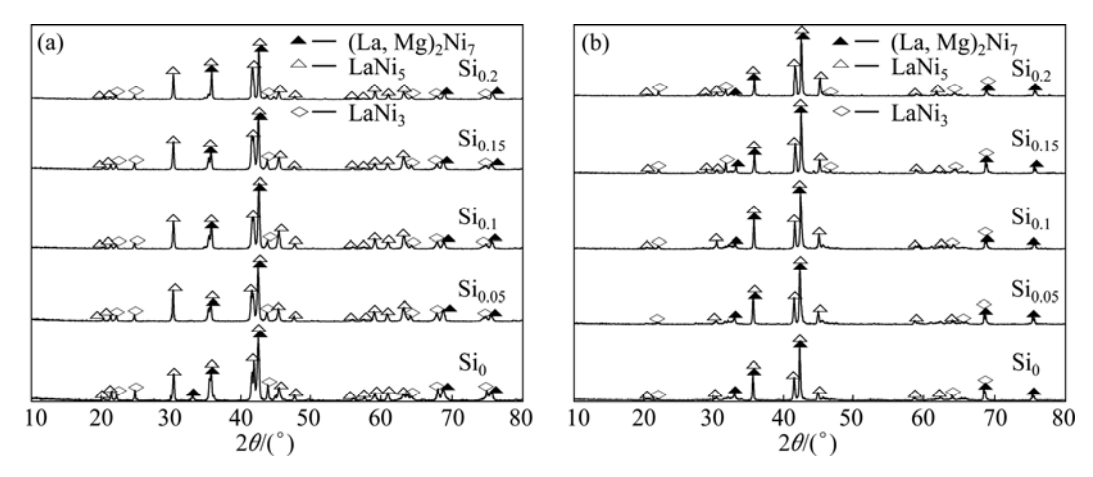


Fig. 1 XRD patterns of as-cast (a) and as-annealed (b) $La_{0.8}Mg_{0.2}Ni_{3.3}Co_{0.2}Si_x(x=0-0.2)$ alloys

Table 1 Lattice parameters and abundances of major phases (La, Mg)₂Ni₇ and LaNi₅

Condition	Alloy	Major phase	Lattice constant		Cell volume, V/nm ³	D1 1 1 /0/
			a/nm	c/nm	Ceil volume, v/nm	Phase abundance /%
As-cast	Si_0	$(La, Mg)_2Ni_7$	0.5062	2.4568	0.5452	73.2
		LaNi ₅	0.5037	0.4002	0.0879	22.6
	$\mathrm{Si}_{0.05}$	$(La, Mg)_2Ni_7$	0.5063	2.4568	0.5454	70.1
		LaNi ₅	0.5042	0.4009	0.0883	25.2
	$Si_{0.1}$	$(La, Mg)_2Ni_7$	0.5064	2.4569	0.5456	66.7
		LaNi ₅	0.5049	0.4014	0.0886	28.2
	Si _{0.15}	$(La, Mg)_2Ni_7$	0.5064	2.4571	0.5457	61.4
		LaNi ₅	0.5053	0.4019	0.0889	33.3
	$\mathrm{Si}_{0.2}$	$(La, Mg)_2Ni_7$	0.5065	2.4572	0.5459	55.7
		LaNi ₅	0.5059	0.4023	0.0892	38.4
As-annealed (900 °C)	Si_0	$(La, Mg)_2Ni_7$	0.5065	2.4569	0.5458	76.2
		LaNi ₅	0.5040	0.4006	0.0881	19.6
	$\mathrm{Si}_{0.05}$	$(La, Mg)_2Ni_7$	0.5065	2.4570	0.5459	73.1
		LaNi ₅	0.5044	0.4012	0.0884	22.2
	Si _{0.1}	$(La, Mg)_2Ni_7$	0.5067	2.4571	0.5463	69.7
		LaNi ₅	0.5051	0.4017	0.0888	25.2
	Si _{0.15}	(La, Mg) ₂ Ni ₇	0.5068	2.4573	0.5466	64.4
		LaNi ₅	0.5055	0.4023	0.0890	30.3
	Si _{0.2}	(La, Mg) ₂ Ni ₇	0.5068	2.4574	0.5466	58.7
		LaNi ₅	0.5062	0.4027	0.0894	35.4

phase is evidently higher than that in $(La, Mg)_2Ni_7$ phase, which conforms very well to the results of the XRD observation. Apparently, the morphologies of the as-cast and as-annealed Si_0 and $Si_{0.2}$ alloys display a dendrite structure. The annealing treatment turns out an obvious homogeneity of the composition segregation in the alloys.

3.2 Electrochemical hydrogen storage performances

3.2.1 Activation capability and discharge capacity

The number of charging-discharging cycles, which is required for attaining the greatest discharge capacity

through the cycle at a constant current density of 60 mA/g, is used to characterize the activation capability of an alloy electrode. The smaller the number of charging—discharging cycles is, the better the activation property will be. Figure 3 describes the variations of the discharge capacities of the as-cast and as-annealed La_{0.8}Mg_{0.2}Ni_{3.3}Co_{0.2}Si_x (x=0-0.2) alloys with the cycle number. It indicates that almost all the alloys reach their maximum discharge capacities at the first charging—discharging cycle, exhibiting an excellent activation performance. Whether adding Si or annealing treatment does not affect the activation capability of the alloy.

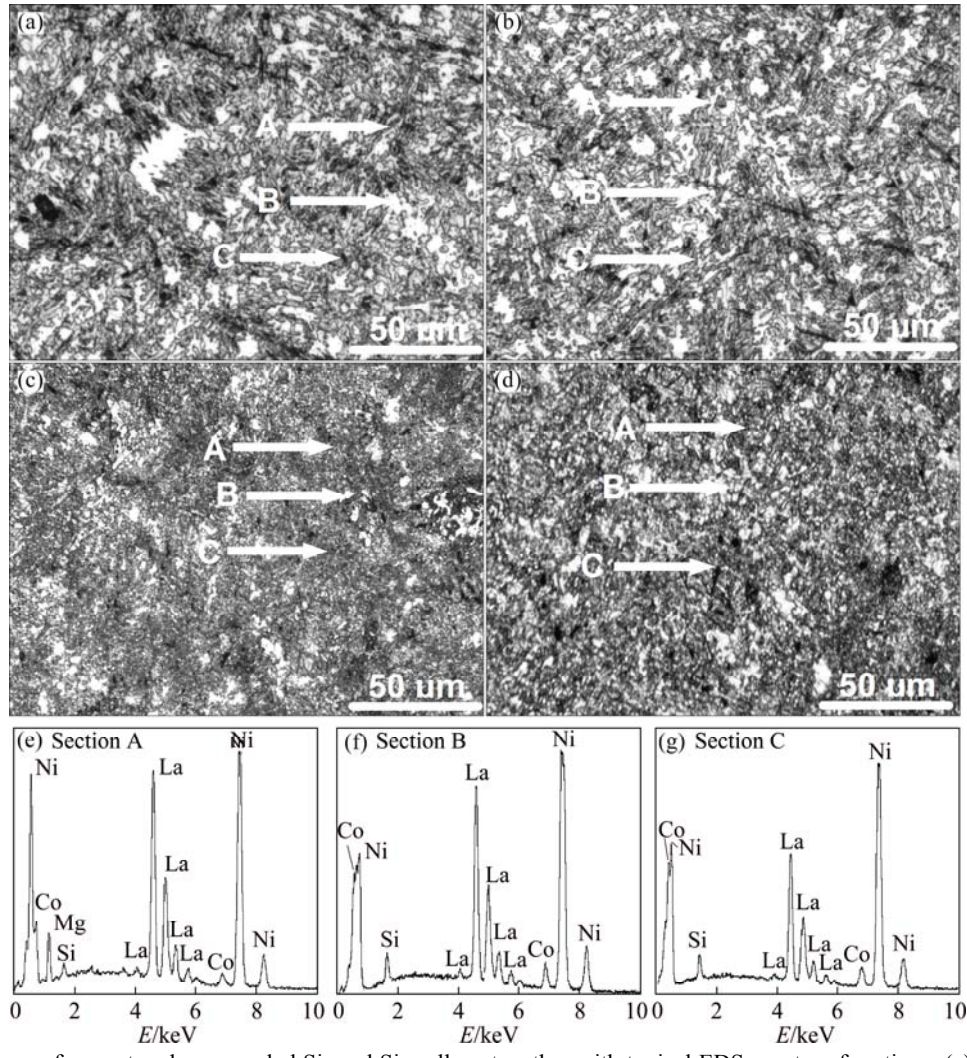


Fig. 2 SEM images of as-cast and as-annealed Si_0 and $Si_{0.2}$ alloys together with typical EDS spectra of sections: (a) SEM images of as-cast Si_0 alloy; (b) SEM image of as-cast Si_0 alloy; (c) SEM image of as-annealed Si_0 alloy; (d) SEM image of as-annealed Si_0 alloy; (e) EDS of section A; (f) EDS of section B; (g) EDS of section C

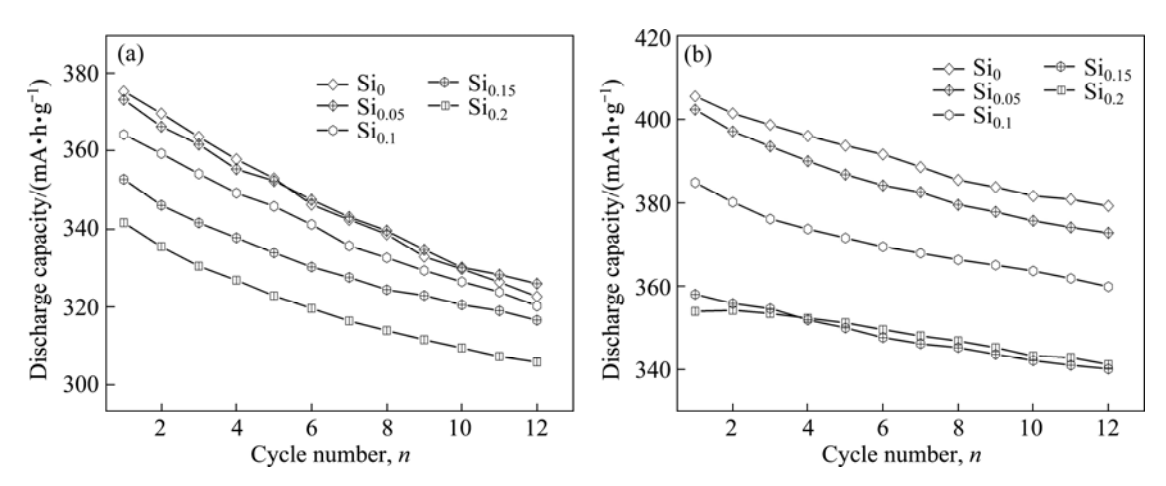


Fig. 3 Evolution of discharge capacity of $La_{0.8}Mg_{0.2}Ni_{3.3}Co_{0.2}Si_x(x=0-0.2)$ alloys with cycle number: (a) As-cast; (b) As-annealed

Figure 4 demonstrates the evolution of the discharge capacity of the as-cast and as-annealed $La_{0.8}Mg_{0.2}Ni_{3.3}Co_{0.2}Si_x$ (x=0-0.2) alloys with Si content. Obviously, the addition of Si gives rise to an evident

decrease in the discharge capacity. With the Si content increasing from 0 to 2, the discharge capacity declines from 375.5 to 341.6 mA·h/g for the as-cast alloy, and from 405.5 to 354.1 mA·h/g for the as-annealed alloy.

Also, it is found that, for the same Si content, the as-annealed alloy exhibits a much higher discharge capacity than that of the as-cast one.

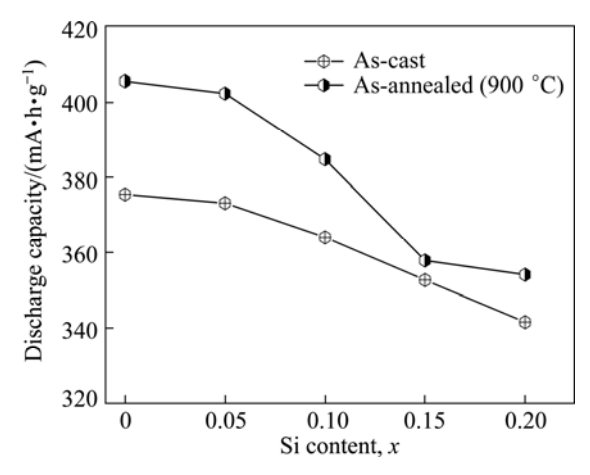


Fig. 4 Evolution of discharge capacity of as-cast and as-annealed $La_{0.8}Mg_{0.2}Ni_{3.3}Co_{0.2}Si_x$ (x=0-0.2) alloys with Si content x

As a matter of fact, the activation capability of an alloy electrode is believed to be associated with the change of the internal energy of the hydride system before and after hydrogen absorption. The larger the added internal energy which involves the surface energy originated from oxidative film forming on the electrode alloy surface and the stain energy produced by hydrogen atom entering the interstitial of the tetrahedron or octahedron of the alloy lattice is, the poorer the activation performance of the alloy will be [13]. The superior activation performance of the as-cast and as-annealed alloys is mainly ascribed to their multiphase structures because lots of phase boundaries can decrease the lattice distortion and the strain energy formed in the process of hydrogen absorption. Furthermore, the phase boundaries also provide good diffusion tunnels for hydrogen atoms, improving the activation performance of the alloy. The addition of Si enlarges the cell volume and decreases the expansion/contraction ratio of the alloy in the process of the hydrogen absorption/desorption, meaning that the strain energy becomes small.

With respect to the discharge capacity of the alloy electrode, it is determined by multiple factors, involving crystal structure, phase component and constitution, grain size, composition uniformity and surface state, etc. The reduced discharge capacity of alloys incurred by adding Si can be ascribed to the following reasons. Firstly, the addition of Si makes the discharge capacity of the LaNi₅ phase significantly decrease, which has been recognized deeply [14–16]. Secondly, the reduction of the (La, Mg)₂Ni₇ phase caused by adding Si is detrimental to the discharge capacity because the (La, Mg)₂Ni₇ phase possesses much higher electrochemical

capacity than the LaNi $_5$ phase. The annealing treatment makes the discharge capacity of the alloys considerably increase which is attributed to the homogenization of the composition and the changes of the phase abundance as well as the lattice parameters originated by annealing treatment.

3.2.2 Electrochemical cycle stability

The cycle stability of the electrode alloy, a decisive factor for the life of the Ni-MH battery, is evaluated by capacity retaining rate (S_n) , which is defined as $S_n = C_n/C_{\text{max}} \times 100\%$, where C_{max} is the maximum discharge capacity and C_n is the discharge capacity at the nth charge-discharge cycle with a current density of 300 mA/g, respectively. Figure 5 provides the variations of the S_n values of the as-cast and as-annealed $La_{0.8}Mg_{0.2}Ni_{3.3}Co_{0.2}Si_x$ (x=0-0.2) alloys depending on the charge-discharge cycle number. Evidently, the slopes of the curves, qualitatively reflecting the degradation rate of the discharge capacity during the charge-discharge cycle, markedly decline with the rising of Si content, implying that the addition of Si engenders a positive impact on the cycle stability of the alloy. In order to quantitatively describe the effects of Si content on the cycle stability of the alloy, the evolution of the capacity retaining rate S_{100} (at the 100th cycle) of the La_{0.8}Mg_{0.2}Ni_{3.3}Co_{0.2}Si_x

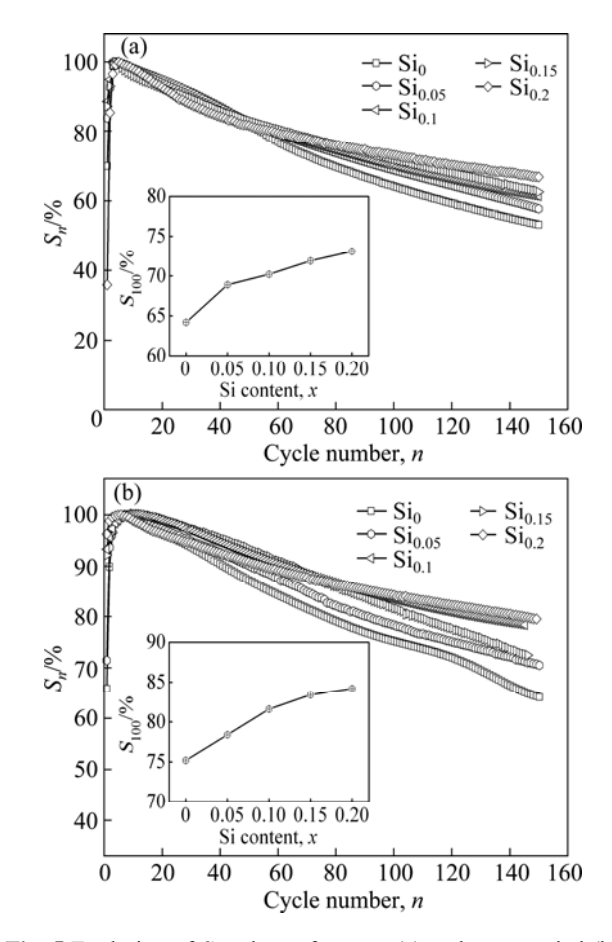


Fig. 5 Evolution of S_n values of as-cast (a) and as-annealed (b) $La_{0.8}Mg_{0.2}Ni_{3.3}Co_{0.2}Si_x(x=0-0.2)$ alloys with cycle number

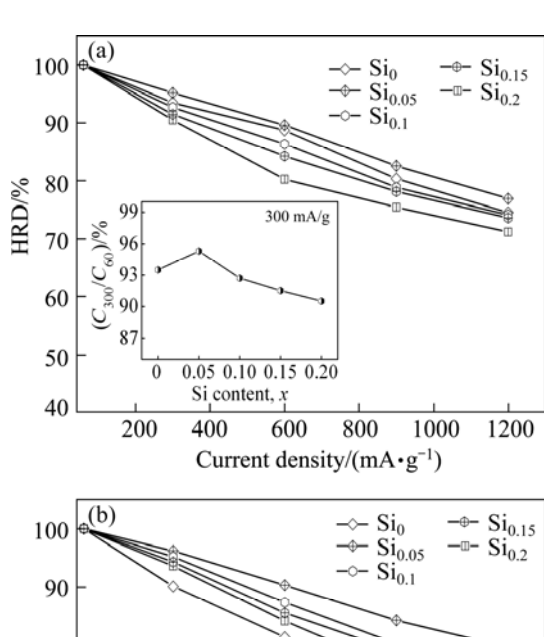
(x=0-0.2) alloys with Si content, which acts as a criterion, is given in Fig. 5 too. We find that the S_{100} values visibly rise with the growing of Si content, and are enhanced from 64.2% to 73.1% for the as-cast alloy and from 75.2% to 84.2% for the as-annealed one accompanying Si content increasing from 0 to 0.2. Noticeably, the S_{100} values of the as-annealed alloys are much higher than those of the as-cast ones, indicating that the annealing treatment plays a positive role in the cycle stability.

As a matter of fact, the final invalidation of an alloy electrode is caused by the accumulation of the discharge capacity decay, which is unavoidable during the charge-discharge cycles. It is well known that the degradation of the discharge capacity of the A₂B₇-type alloy electrode results from the ever-thickening Mg(OH)₂ and La(OH)₃ surface layers, which hinder the hydrogen atoms from diffusing in or out, in alkaline solutions [17]. Moreover, the hydrogen storage material suffers a volume change during the charge-discharge process which aggravates the cracking and pulverizing of the alloy, and then makes the surface of the material apt to be oxidized. Therefore, the positive impact of the additive Si on the cycle stability of the alloy is ascribed to several aspects as follows. Firstly, the added Si generates a passivated silicon oxide layer on the surface of the alloy electrode [15,18] which effectively protects it from being corroded. Secondly, the increased LaNi₅ phase induced by adding Si raises the cycle stability due to an inarguable fact that the LaNi₅ phase possesses a stable property much superior to the (La, Mg)₂Ni₇ phase in cyclic lives. Thirdly, the enlarged cell volume on account of adding Si decreases the ratios of expansion/contraction in the process of hydrogen absorption/desorption, enhancing the anti-pulverization capability. At the same time, the annealing brings about some other salutary contributions for the alloy such as the structure change and the more homogeneous composition distribution, which also facilitate to prohibit the pulverization and corrosion of the alloy, thus making the alloy's cycle stability raise [19].

3.2.3 Electrochemical hydrogen storage kinetics

The electrochemical hydrogen storage kinetics, regarded to be a comparable factor with discharge capacity and cycle stability, is symbolized by its high rate discharge ability (HRD) which is calculated as follows: HRD= $C_{i,\text{max}}/C_{60,\text{max}} \times 100\%$, where $C_{i,\text{max}}$ and $C_{60,\text{max}}$ are the maximum discharge capacities of the alloy electrode charged–discharged at the current densities of i and 60 mA/g respectively. The variations of HRD values of the as-cast and as-annealed La_{0.8}Mg_{0.2}Ni_{3.3}Co_{0.2}Si_x (x=0–0.2) alloys depending on the discharge current density are illustrated in Fig. 6. It is found that the addition of Si gives rise to an evident impact on the HRD

of the alloy. In order to describe the influence of Si content more clearly, the evolution of the HRD values (at the fixed current density of 300 mA/g) of these alloys with Si content varying is also inserted in Fig. 6. Evidently, the as-cast and as-annealed alloys yield the largest HRD values, namely 95.3% and 96.2%, respectively, when the content of Si is 0.05.



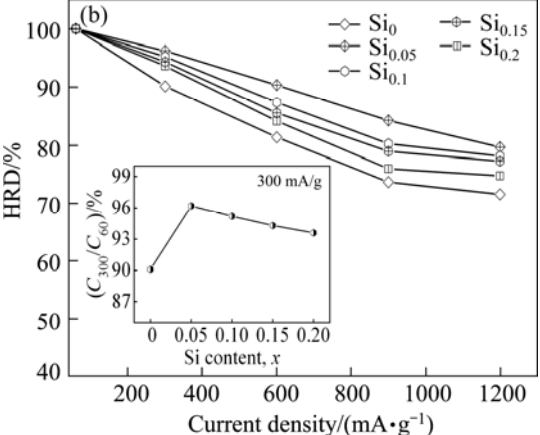


Fig. 6 Evolution of HRD values of as-cast (a) and as-annealed (b) $La_{0.8}Mg_{0.2}Ni_{3.3}Co_{0.2}Si_x$ (x=0-0.2) alloys with discharge current density

The electrochemical hydriding/dehydriding reaction taking place at the hydrogen storage electrode in an alkaline solution during charging and discharging process can be expressed by the following equation:

$$M + \frac{x}{2}H_2O + \frac{x}{2}e \Longrightarrow MH_x + \frac{x}{2}OH^-$$
 (1)

where M is the hydrogen storage alloy. The hydrogen atoms adhered to the grain surface of the alloy electrode have two final whereabouts, forming hydrogen molecule or diffusing into the bulk alloy and forming metallic hydrides. That is to say, the diffusion rate of hydrogen atom within the surface layer of alloy determines the utilization of charging current, which is just the ratio of the diffusion current to the imposing current. It is universally agreed that the electrochemical hydrogen

kinetics of the alloy electrode is determined by the hydrogen diffusion capability in the alloy bulk and the charge-transfer rate on the surface of an alloy electrode [20]. Thereby, it is extremely important to investigate the hydrogen diffusion coefficient and the charge-transfer rate. The diffusion coefficients of hydrogen atoms can be obtained by measuring the semilogarithmic curves of anodic current versus working duration of an alloy, as given in Fig. 7. According to the model established by ZHENG et al [21], the diffusion coefficient of the hydrogen atoms in the bulk of the alloy could be calculated through the slope of the linear region of the corresponding plots by the following formulae:

$$\lg J = \lg \left(\pm \frac{6FD}{da^2} (C_0 - C_s) \right) - \frac{\pi^2}{2.303} \frac{D}{a^2} t$$
 (2)

$$D = -\frac{2.303a^2}{\pi^2} \frac{d \lg J}{dt}$$
 (3)

where J is the diffusion current density, F is the Faraday constant, D is the hydrogen diffusion coefficient, C_0 is the initial hydrogen concentration in the bulk of the alloy, C_s is the hydrogen concentration on the surface of the alloy particles, a is the alloy particle radius, d is the

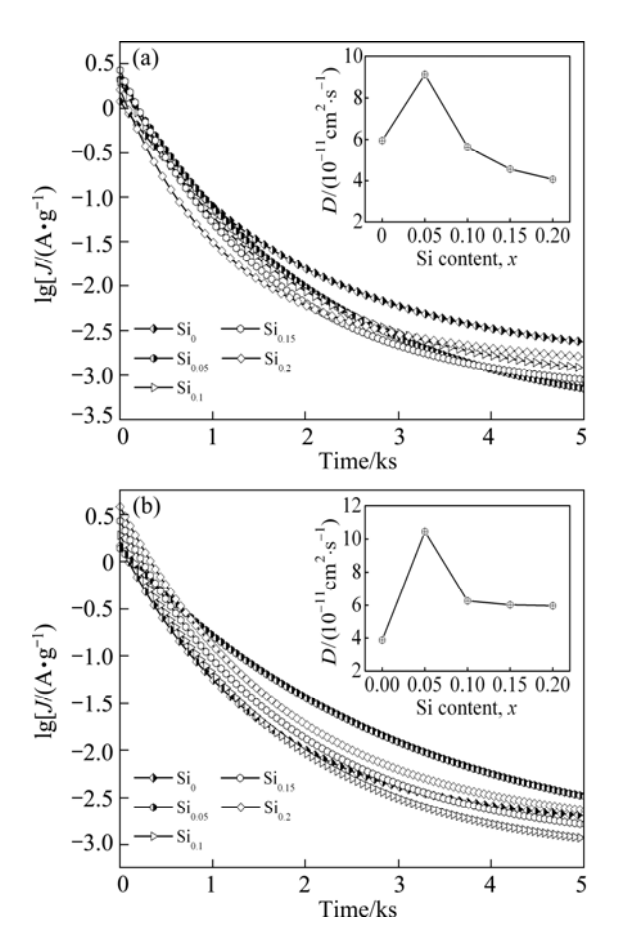


Fig. 7 Semi-logarithmic curves of anodic current vs time responses of as-cast (a) and as-annealed (b) $La_{0.8}Mg_{0.2}Ni_{3.3}Co_{0.2}Si_x(x=0-0.2)$ alloys

density of the hydrogen storage alloy, and t is the discharge time. The variations of the hydrogen diffusion coefficient D calculated by Eq. (3) with Si content are also inserted in Fig. 7. It exhibits that the D values of the as-cast and as-annealed alloys first increase and then decrease with Si content rising, suggesting that the diffusion coefficient of hydrogen atoms is an important factor dominating the electrochemical kinetics of the alloy.

To ascertain the kinetics of electrochemical absorption/desorption, Tafel polarization hydrogen curves of the as-cast and as-annealed $La_{0.8}Mg_{0.2}Ni_{3.3}Co_{0.2}Si_x(x=0-0.2)$ alloys are measured, as shown in Fig. 8. A clear point of inflection appears in each anodic polarization curve, implying the existence of critical value which is termed as limiting current density $(J_{\rm L})$. This indicates that an oxidation reaction takes place on the surface of the alloy electrode, and the generated oxidative product hinders further penetration of hydrogen atoms [22]. Thereby the limiting current density can be viewed as a critical current density of passivation, which is mainly determined by the solid state diffusion of hydrogen in metal-hydride electrode [23]. The J_L values of the as-cast and as-annealed $La_{0.8}Mg_{0.2}Ni_{3.3}Co_{0.2}Si_x$ (x=0-0.2) alloys as a function of

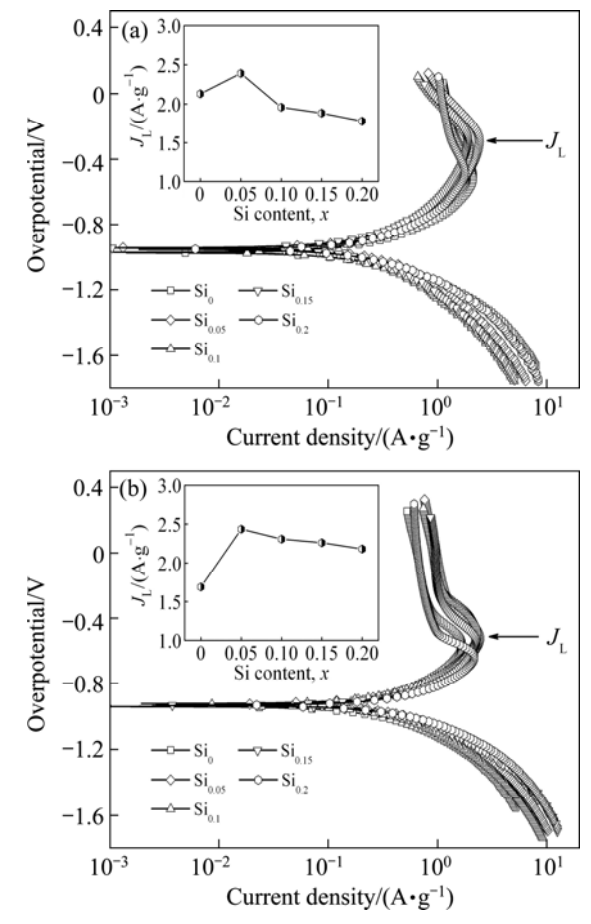


Fig. 8 Tafel polarization curves of as-cast (a) and as-annealed (b) $La_0 {}_8Mg_0 {}_2Ni_3 {}_3Co_0 {}_2Si_x (x=0-0.2)$ alloys

Si content are also presented in Fig. 8. Obviously, the $J_{\rm L}$ values of the as-cast and as-annealed alloys first mount up then go down with the rising of Si content, obtaining their maximum values when Si content is 0.05 where the alloys attain the largest HRD values too, once again proving that the hydrogen diffusion ability in the alloy bulk is a pivotal factor of the electrochemical kinetics of the alloys.

The charge-transfer ability on the surface of an alloy electrode is qualitatively evaluated by its electrochemical impedance spectrum (EIS), and EIS curves of as-cast as-annealed the and $La_{0.8}Mg_{0.2}Ni_{3.3}Co_{0.2}Si_x$ (x=0-0.2) alloys are illustrated in Fig. 9. Clearly, each EIS spectrum comprises two distorted capacitive loops at high and middle frequencies as well as an almost straight line at low frequencies, which exactly represent the electrochemical processes just as interpreted and modeled by KURIYAMA et al [24]. The smaller semicircle in the high frequency region corresponds to the contact resistance between the alloy powder and the conductive material, and the larger one in the middle frequency region equates to the charge-transfer resistance on the alloy surface while the straight line in low frequency relates to the atomic hydrogen diffusion in the alloy. It is very obvious that the larger the radius of the semicircle in the middle frequency region is, the higher the charge-transfer resistance of the alloy electrode will be. From Fig. 9, we can see that the radii of the large semicircles of the as-cast and as-annealed alloys in the middle frequency

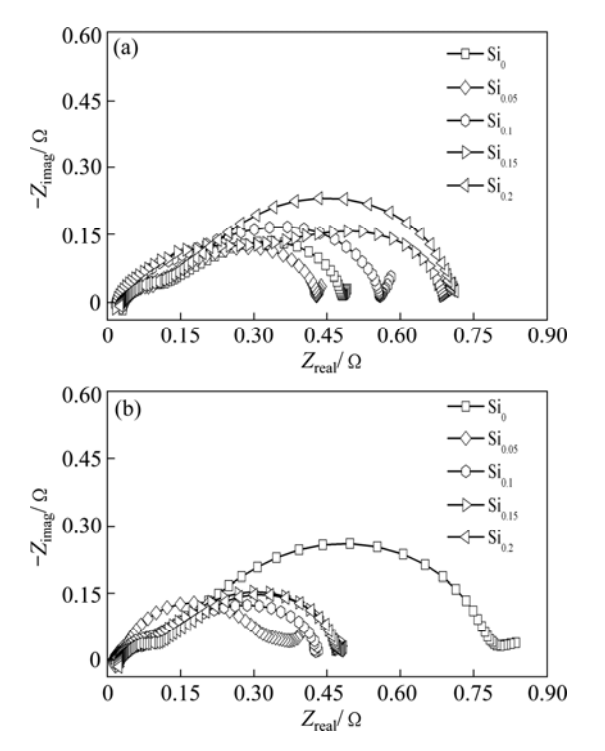


Fig. 9 Electrochemical impedance spectra (EIS) of as-cast (a) and as-annealed (b) $La_{0.8}Mg_{0.2}Ni_{3.3}Co_{0.2}Si_x(x=0-0.2)$ alloys

first shrink and then expand with the rising Si content.

The above-mentioned results reveal that the HRD and the electrochemical kinetics of the as-cast and as-annealed alloys first augment and then minish with the rising of Si content, implying that the addition of Si causes influence of both positive and negative aspects on the electrode hydrogen storage kinetics. The positive contribution exhibits two directions: Firstly, the increase of the LaNi₅ phase dramatically improves the electrocatalytic activity of the alloy electrodes; Secondly, the enlargement of cell volume lessens the diffusion activating energy of hydrogen atoms. Both of above factors are beneficial to the improvement of the alloy's HRD. The negative action results from the compact silicon oxide layer generated by adding Si, which not only severely impairs the charge-transfer rate on the alloy surface but also hinders the hydrogen diffusion from inner of the bulk to the surface, subsequently giving rise to the drop of the electrochemical kinetic property. It is the above-mentioned contrary impact engendered by adding Si, yielding a maximum HRD value of the alloy.

4 Conclusions

- 1) The addition of Si gives an increase in the $LaNi_5$ phase and a decrease in the (La, $Mg)_2Ni_7$ phase of the alloys instead of altering their phase structures and such addition also incurs a visible increment in the lattice constants and cell volume of the alloys.
- 2) All the as-cast and as-annealed alloys possess a superior activation capability, on which the addition of Si makes few impacts. The addition of Si lowers the discharge capacities of the as-cast and as-annealed alloys, while enhancing their cycle stabilities markedly. The HRD values of the as-cast and as-annealed alloys first increase and then decrease with the rising Si content, to which a rather similar trend is obtained by measuring the hydrogen diffusion coefficient, Tafel polarization curves and electrochemical impedance spectra (EIS).
- 3) The annealing treatment also improves the discharge capacity and cycle stability visibly, for which the more homogeneous composition distribution and the structural change after being annealed are principally responsible.

References

- [1] BENCZUR-ÜRMÖSSY G, BERTHOLD D O M, WIESENER K. Batteries for portable applications and electric vehicles [C]//The electrochemical society proceedings series. New Jersey: Pennington, 1997: 869–874.
- [2] KADIR K, SAKAI T, UEHARA I. Synthesis and structure determination of a new series of hydrogen storage alloys: RMg₂Ni₉ (R=La, Ce, Pr, Nd, Sm and Gd) built from MgNi₂ Laves-type layers alternating with AB₅ layers [J]. Journal of Alloys and Compounds, 1997, 257: 115–121.

- [3] KOHNO T, YOSHIDA H, KAWASHIMA F, INABA T, SAKAI I, YAMAMOTO M, KANDA M. Hydrogen storage properties of new ternary system alloys: La₂MgNi₉, La₅Mg₂Ni₂₃, La₃MgNi₁₄ [J]. Journal of Alloys and Compounds, 2000, 311: L5-L7.
- [4] LIU Y F, PAN H G, GAO M X, WANG Q D. Advanced hydrogen storage alloys for Ni/MH rechargeable batteries [J]. Journal of Materials Chemistry, 2011, 21: 4743–4755.
- [5] LIU Y F, CAO Y H, HUANG L, GAO M X, PAN H G. Rare earth–Mg–Ni-based hydrogen storage alloys as negative electrode materials for Ni/MH batteries [J]. Journal of Alloys and Compounds, 2011, 509: 675–686.
- [6] LIU Y F, PAN H G, GAO M X, LI R, LEI Y Q. Effect of Co content on the structural and electrochemical properties of the La_{0.7}Mg_{0.3}Ni_{3.4-x}Mn_{0.1}Co_x hydride alloys: II. Electrochemical properties [J]. Journal of Alloys and Compounds, 2004, 376: 304–313.
- [7] ZHANG Y H, LI B W, REN H P, CAI Y, DONG X P, WANG X L. Cycle stabilities of the La_{0.7}Mg_{0.3}Ni_{2.55-x}Co_{0.45}M_x (M=Fe, Mn, Al; x=0, 0.1) electrode alloys prepared by casting and rapid quenching [J]. Journal of Alloys and Compounds, 2008, 458: 340–345.
- [8] ZHANG Y H, LI B W, REN H P, WU Z W, DONG X P, WANG X L. Investigation on structures and electrochemical characteristics of the as-cast and quenched La_{0.5}Ce_{0.2}Mg_{0.3}Co_{0.4}Ni_{2.6-x}Mn_x (x=0-0.4) electrode alloys [J]. Journal of Alloys and Compounds, 2008, 461: 591-597.
- [9] SHEN X Q, CHEN Y G, TAO M D, WU C L, DENG G, KANG Z Z. The structure and high-temperature (333 K) electrochemical performance of La_{0.8-x}Ce_xMg_{0.2}Ni_{3.5} (x=0.00-0.20) hydrogen storage alloys [J]. International Journal of Hydrogen Energy, 2009, 34: 3395-3403.
- [10] ZHANG Y H, LI B W, REN H P, GUO S H, QI Y, WANG X L. Structures and electrochemical hydrogen storage characteristics of La_{0.75-x}Pr_xMg_{0.25}Ni_{3.2}Co_{0.2}Al_{0.1} (x=0-0.4) alloys prepared by melt spinning [J]. Journal of Alloys and Compounds, 2009, 485: 333-339.
- [11] SHEN X Q, CHEN Y G, TAO M D, WU C L, DENG G, KANG Z Z.

 The structure and 233 K electrochemical properties of La_{0.8-x}Nd_xMg_{0.2}Ni_{3.1}Co_{0.25}Al_{0.15} (x=0.0-0.4) hydrogen storage alloys [J]. International Journal of Hydrogen Energy, 2009, 34: 2661–2669.
- [12] LIU Y F, PAN H G, YUE Y J, WU X F, CHEN N, LEI Y Q. Cycling durability and degradation behavior of La–Mg–Ni–Co-type metal hydride electrodes [J]. Journal of Alloys and Compounds, 2005, 395: 291–299.
- [13] SIMIČIĆ M V, ZDUJIĆ M, DIMITRIJEVIĆ R, NIKOLIĆ-BUJANOVIĆ L, POPOVIĆ N H. Hydrogen absorption and electrochemical properties of Mg₂Ni-type alloys synthesized by

- mechanical alloying [J]. Journal of Power Sources, 2006, 158: 730-734.
- [14] MELI F, ZUETTEL A, SCHLAPBACH L. Surface and bulk properties of LaNi_{5-x}Si_x alloys from the viewpoint of battery applications [J]. Journal of Alloys and Compounds, 1992, 190: 17-24
- [15] WILLEMS J J G. Metal hydride electrodes stability of LaNi₅-related compounds [J]. Philips J Res, 1984, 39: 1–94.
- [16] SAKAI T, OGURO K, MIYAMURA H, KURIYAMA N, KATO A, ISHIKAWA H, IWAKURA C. Some factors affecting the cycle lives of LaNi₅-based alloy electrodes of hydrogen batteries [J]. Journal of the Less-Common Metals, 1990, 161: 193–202.
- [17] DORNHEIM M, DOPPIU S, BARKHORDARIAN G, BOESENBERG U, KLASSEN T, GUTFLEISCH O, BORMANN R. Hydrogen storage in magnesium-based hydrides and hydride composites [J]. Scripta Materialia. 2007, 56: 841–846.
- [18] WILLEMS J J G, BUSCHOW K H J. From permanent magnets to rechargeable hydride electrodes [J]. Journal of the Less-Common Metals. 1987, 129: 13–30.
- [19] PAN H G, CHEN N, GAO M X, LI R, LEI Y Q, WANG Q D. Effects of annealing temperature on structure and the electrochemical properties of La_{0.7}Mg_{0.3}Ni_{2.45}Co_{0.75}Mn_{0.1}Al_{0.2} hydrogen storage alloy [J]. Journal of Alloys and Compounds, 2005, 397: 306–312.
- [20] RATNAKUMAR B V, WITHAM C, BOWMAN R C Jr, HIGHTOWER A, FULTZ B. Electrochemical studies on LaNi $_{5-x}$ Sn $_x$ metal hydride alloys [J]. Journal of the Electrochemical Society, 1996, 143: 2578–2584.
- [21] ZHENG G, POPOV B N, WHITE R E. Electrochemical determination of the diffusion coefficient of hydrogen through a LaNi_{4.25}Al_{0.75} electrode in alkaline aqueous solution [J]. Journal of the Electrochemical Society, 1995, 142: 2695–2698.
- [22] ZHAO X Y, DING Y, MA L Q, WANG L Y, YANG M, SHEN X D. Electrochemical properties of MmNi_{3.8}Co_{0.75}Mn_{0.4}Al_{0.2} hydrogen storage alloy modified with nanocrystalline nickel [J]. International Journal of Hydrogen Energy, 2008, 33: 6727–6733.
- [23] LIU Y F, PAN H G, GAO M X, ZHU Y F, LEI Y Q, WANG Q D. The effect of Mn substitution for Ni on the structural and electrochemical properties of La_{0.7}Mg_{0.3}Ni_{2.55-x}Co_{0.45}Mn_x hydrogen storage electrode alloys [J]. International Journal of Hydrogen Energy, 2004, 29: 297–305.
- [24] KURIYAMA N, SAKAI T, MIYAMURA H, UEHARA I, ISHIKAWA H, IWASAKI T. Electrochemical impedance and deterioration behavior of metal hydride electrodes [J]. Journal of Alloys and Compounds, 1993, 202: 183–197.

添加 Si 对 A_2B_7 型电极合金结构及电化学贮氢性能的影响

张羊换^{1,2}, 任慧平¹, 蔡 颖¹, 杨 泰 ^{1,2}, 张国芳 ^{1,2}, 赵栋梁 ²

- 1. 内蒙古科技大学 内蒙古自治区白云鄂博矿多金属资源综合利用重点实验室,包头 014010;
 - 2. 钢铁研究总院 功能材料研究所, 北京 100081

摘 要:为改善 La_-Mg_-Ni 系 A_2B_7 型合金的电化学贮氢性能,在合金中添加一定量的 Si 元素,通过真空熔炼及退火处理的方法制备 $La_{0.8}Mg_{0.2}Ni_{3.3}Co_{0.2}Si_x$ (x=0-0.2)电极合金。研究 Si 元素的添加对合金结构及电化学贮氢性能的影响。结果表明,铸态及退火态合金均为多相结构,分别为 Ce_2Ni_7 型的(La_i Mg_2Ni_7 相和 $CaCu_5$ 型的 $LaNi_5$ 相以及少量的残余相 $LaNi_3$ 。Si 元素的添加没有改变合金的主相,但使得合金中的(La_i Mg_2Ni_7 相减少而 $LaNi_5$ 相增加。添加 Si 显著地影响了合金的电化学性能。随着 Si 含量的增加,铸态及退火态合金的放电容量逐步降低,但循环稳定性却随着 Si 含量的增加而增强。此外,合金电极的高倍率放电性能、极限电流密度、氢扩散系数以及电化学交流阻抗谱的测试均表明合金的电化学动力学性能随着 Si 含量的增加先增加而后减小。

关键词: A₂B₇型电极合金;添加 Si;结构;电化学性能